

Temporal coherence of optical fields in the presence of entanglement

Yunxiao Zhang,¹ Nan Huo,¹ Liang Cui,¹ Xueshi Guo,¹ Jiahao Fan,² Zhedong Zhang,² Xiaoying Li,^{1, a)} and Z. Y. Ou^{2, b)}

¹⁾ College of Precision Instrument and Opto-Electronics Engineering, Key Laboratory of Opto-Electronics Information Technology, Ministry of Education, Tianjin University, Tianjin 300072, P. R. China

²⁾ Department of Physics, City University of Hong Kong, 83 Tat Chee Avenue, Kowloon, Hong Kong, P. R. China

In classical coherence theory, coherence time is typically related to the bandwidth of the optical field. Narrowing the bandwidth will result in the lengthening of the coherence time. This will erase temporal distinguishability of photons due to time delay in pulsed photon interference. However, this is changed in an SU(1,1)-type quantum interferometer where quantum entanglement is involved. In this paper, we investigate how the temporal coherence of the fields in a pulse-pumped SU(1,1) interferometer changes with the bandwidth of optical filtering. We find that, because of the quantum entanglement, the coherence of the fields does not improve when optical filtering is applied, in contrary to the classical coherence theory, and quantum entanglement plays a crucial role in quantum interference in addition to distinguishability.

In quantum mechanics, indistinguishability is a fundamental concept for quantum interference. When there exist distinguishable paths for two interfering fields, no interference can occur. This is at the heart of Bohr's complementarity principle for quantum interference¹ and is summarized quantitatively in a relation as^{2,3}

$$\mathcal{V}^2 + \mathcal{D}^2 \leq 1 \quad (1)$$

between the visibility of interference \mathcal{V} and the path distinguishability \mathcal{D} . On the other hand, path distinguishability can be erased by projection measurement in quantum erasers^{4,5}. This erasure of distinguishability can also be achieved in the measurement process. For example, optical filtering can increase the coherence time of an optical field. In an interference experiment involving optical pulses, when optical delay is introduced to achieve distinguishability in time, no interference occurs by direct detection. But placing a narrow band filter in front of the detector can erase the temporal distinguishability by lengthening the pulse and recover the interference effect. This is what leads to the important concept of coherence time in classical coherence theory. It is the time interval in which an optical field keeps its phase correlation and according to the classical coherence theory, it is typically related to the reciprocal bandwidth of an optical field⁶ and can be lengthened by optical filtering. Indeed, a Gaussian-shaped field passing through a filter of Gaussian profile of width σ_f has its coherence time changed to (see Supplementary Materials I for details)

$$T'_c = \sqrt{T_c^2 + 1/\sigma_f^2} \quad (2)$$

with T_c as its original coherence time.

On the other hand, quantum entanglement exists for quantum fields, which was recently shown^{7,8} to be the

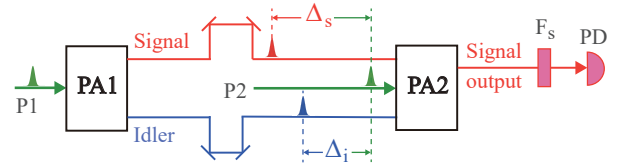


FIG. 1. An unbalanced SU(1,1) interferometer (SUI) with filtered detection. PA, parametric amplifier; P, pump; F_s narrow band filter; PD, power detector.

missing third quantity for Eq.(1) to take the equal sign. With entanglement, Eq.(1) takes the new form of

$$\mathcal{V}^2 + \mathcal{D}^2 + \mathcal{C}^2 = 1, \quad (3)$$

where quantity \mathcal{C} is the concurrence that is a measure of entanglement. The strong quantum correlations between two entangled fields give $\mathcal{C} = 1$ and can thus lead to disappearance of coherence ($\mathcal{V} = 0$) even if there is indistinguishability ($\mathcal{D} = 0$)⁹. Moreover, quantum entanglement makes it possible to manipulate the coherence property of one field by controlling the other entangled field^{10–12}. All this poses a challenge for the aforementioned traditional concept of temporal coherence as related to the reciprocal bandwidth of the field: narrow filtering leads to the temporal indistinguishability but does not deal with entanglement, which can reduce interference effect as well according to Eq.(3).

An SU(1,1) interferometer is a quantum interferometer that is a perfect platform for this study. It utilizes parametric amplifiers (PA) to replace beam splitters in traditional classical interferometers^{13,14}. The signal and idler fields generated in the parametric amplifier are entangled to each other and are used to probe phase changes in the interferometer. Such a novel quantum interferometer has recently been widely applied to quantum imaging¹⁵, quantum sensing^{16–19}, quantum state engineering^{20,21}, and quantum measurement^{22–24}. Because of the involvement of quantum entanglement in the interferometer, its properties can be quite different from traditional classical

^{a)} Electronic mail: xiaoyingli@tju.edu.cn

^{b)} Electronic mail: jefjou@cityu.edu.hk

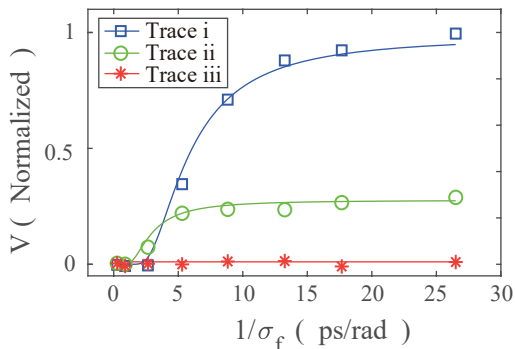


FIG. 2. Visibility as a function of reciprocal bandwidth of the filter. (i) $\Delta_i = 0, \Delta_s = 10ps$; (ii) $\Delta_i = 5ps, \Delta_s = 10ps$; (iii) $\Delta_i = 10ps, \Delta_s = 10ps$.

interferometer²⁵, especially when it concerns the temporal coherence of the fields involved.

For studying this, we consider a pulse-pumped SU(1,1) interferometer shown in Fig.1. The pumps of two PAs, P1 and P2, are originated from the same laser. When the paths are carefully balanced for all the fields involved, interference is observed in both outputs. Because of symmetry, we only need to consider detection at one output, say, the signal port. We now introduce delays (Δ_s, Δ_i) in either of the arms so that interference disappears due to temporal distinguishability. We next place narrow optical filters at the signal output port in front of the detector with the intention to lengthen the coherence time and erase the temporal distinguishability. This works for the delay in signal field only ($\Delta_s \neq 0$ but $\Delta_i = 0$), as shown in the blue data points (Trace i) in Fig.2, where the visibility increases with the narrowing of the filter and eventually reaches 100%. But it fails if there is a delay in the idler field ($\Delta_i \neq 0$), as shown in the green (Trace ii) and red (Trace iii) data points in Fig.2 (see Supplementary Materials IV-A and IV-B for details of measurement). Notice especially the large Δ_i delay case (Trace iii) with nearly zero visibility no matter how narrow the filter is. This is in complete contradiction with classical coherence theory and is an example of the influence of quantum entanglement on coherence, as we will see in the following.

Although the increase of the visibility in Fig.2 can be attributed to narrowing of the filter as classical coherence theory, the limiting values of $1/\sigma_f \rightarrow \infty$ can only be understood with the language of Eq.(3) by a single-mode two-photon state in the form of

$$|\Psi\rangle = A_1|s_1, i_1\rangle + A_2|s_2, i_2\rangle, \quad (4)$$

where A_1, A_2 are related to the pump fields of PA1 and PA2, respectively and are normalized: $|A_1|^2 + |A_2|^2 = 1$. s_1, i_1 and s_2, i_2 are the signal and idler modes from two PAs, respectively. Normally, they are distinct and independent. When we align the two idler fields together, depending on the delay in the idler field, the two idler modes will change from totally independent when Δ_i is

much larger than the pulse width to completely identical when $\Delta_i = 0$.

For the latter case when $\Delta_i = 0$, the idler photon states from two PAs are identical: $|i_1\rangle = |i_2\rangle \equiv |i\rangle$ so Eq.(4) becomes

$$|\Psi\rangle(\Delta_i = 0) = (A_1|s_1\rangle + A_2|s_2\rangle) \otimes |i\rangle, \quad (5)$$

which is a product state with no entanglement or concurrence $\mathcal{C} = 0$. Then interference observed at the signal output port is related to the indistinguishability in the signal field between $|s_1\rangle$ and $|s_2\rangle$, which can be altered by the optical filtering of the signal field. This corresponds to the classical case when Eq.(1) takes equal sign and is described by the blue data in Fig.2. The solid blue curve is a normalized Gaussian function with a width given by Eq.(2) (see later for detail).

In the other extreme case when there is a large delay in idler field, $|i_1\rangle$ and $|i_2\rangle$ are well separated and the state in Eq.(4) becomes a time-bin entangled state with maximum entanglement for $A_1 = A_2 = 1/\sqrt{2}$, leading to $\mathcal{C} = 1$ but this also gives $\mathcal{D} = 0$ according to Ref. 9. According to Eq.(3), this should give $\mathcal{V} = 0$, which is indeed what we observed as the red points in Fig.2.

The intermediate case for the green data in Fig.2 can be understood by evaluating concurrence \mathcal{C} for the state in Eq.(4) with $|i_2\rangle$ partially overlapping with $|i_1\rangle$: $|i_2\rangle = \cos\theta|i_1\rangle + \sin\theta|u\rangle$, where $\cos\theta = \langle i_1|i_2\rangle$ and $|u\rangle$ is some state orthonormal to $|i_1\rangle$ and can be obtained from Schmidt method. Working in the space spanned by $\{|s_1\rangle, |s_2\rangle, |i_1\rangle, |u\rangle\}$, we find the concurrence $\mathcal{C} = 2|A_1A_2|\sin\theta$ for the state in Eq.(4) (See Supplementary Materials II). It is straightforward to calculate the visibility for interference between fields s_1, s_2 , yielding $\mathcal{V} = 2|A_1A_2|\cos\theta$ and according to Ref. 9, the distinguishability quantity $\mathcal{D} = ||A_1|^2 - |A_2|^2|$. It can be checked that these values of $\mathcal{V}, \mathcal{C}, \mathcal{D}$ satisfy Eq.(3), confirming the role played by entanglement in interference.

One may attempt to reach a full understanding results in Fig.2 by Eq.(3) but this is very complicated because it involves concurrence of a multi-mode two-photon state in a continuous temporal/spectral space. Nevertheless, we can understand the results by calculating the visibility of interference from the multi-mode two-photon state:

$$|\Phi_2\rangle = \int d\omega_1 d\omega_2 \left[\Phi(\omega_1, \omega_2) e^{i\omega_1 \Delta_s} e^{i\omega_2 \Delta_i} + \Phi'(\omega_1, \omega_2) \right] \times \hat{a}_s^\dagger(\omega_1) \hat{a}_i^\dagger(\omega_2) |vac\rangle \quad (6)$$

where $\Phi(\omega_1, \omega_2), \Phi'(\omega_1, \omega_2)$ are the two-photon wave function for the two-photon states produced by PA1 and PA2 respectively and take the form of $A_p^2 \exp[-(\omega_1 + \omega_2 - 2\omega_{p0})^2 / 4\sigma_p^2] F(\omega_1, \omega_2)$ for a four-wave mixing process²⁶ with a Gaussian-shaped pump spectral profile (peak amplitude A_p , width σ_p , center frequency ω_{p0}) and $F(\omega_1, \omega_2)$ as the phase matching factor depending on nonlinear media. The field at signal output after the filter (F_s) but before the detector is

$$\hat{E}_s(t) = \int d\omega \hat{a}_s(\omega) e^{-i\omega t} f_s(\omega) \quad (7)$$

where $f_s(\omega)$ is the filter amplitude transmission function.

Assume the detector is slow and cannot trace the profile of single pulses. Then the output of the detector is

$$\begin{aligned} i_D &\propto \int d\tau \langle \hat{E}_s^\dagger(\tau) \hat{E}_s(\tau) \rangle \\ &\propto \int d\omega_1 d\omega_2 |f_s(\omega_1)|^2 |\Phi_{eq}(\omega_1, \omega_2)|^2 \end{aligned} \quad (8)$$

with $\Phi_{eq}(\omega_1, \omega_2) \equiv \Phi(\omega_1, \omega_2)e^{i\omega_1\Delta_s + i\omega_2\Delta_i} + \Phi'(\omega_1, \omega_2)$.

Assume the two PAs are identical and there is a delay of Δ_p for the pump of PA2 with respect to PA1. Then, $\Phi'(\omega_1, \omega_2) = \Phi(\omega_1, \omega_2)e^{i(\omega_1 + \omega_2)\Delta_p}$ and $|\Phi_{eq}(\omega_1, \omega_2)|^2 = |\Phi(\omega_1, \omega_2)|^2 |e^{i\omega_1(\Delta_s - \Delta_p)} e^{i\omega_2(\Delta_i - \Delta_p)} + 1|^2$. So, if we treat Δ_s, Δ_i as delays reference to the pump of PA2, we can drop Δ_p . Then we have from Eq.(8)

$$\begin{aligned} i_D &\propto \int d\omega_1 d\omega_2 |f_s(\omega_1)|^2 |\Phi(\omega_1, \omega_2)|^2 |e^{i\omega_1\Delta_s} e^{i\omega_2\Delta_i} + 1|^2 \\ &\propto 1 + \mathcal{V}(\Delta_s, \Delta_i) \cos(\omega_{10}\Delta_s + \omega_{20}\Delta_i), \end{aligned} \quad (9)$$

where ω_{10} is the center frequency of the filter for the signal field and with ω_{p0} as the center frequency of the pump field, $\omega_{20} = \omega_{p0} - \omega_{10}$ is the center frequency of the idler field. So, interference is exhibited with visibility

$$\begin{aligned} \mathcal{V}(\Delta_s, \Delta_i) &\equiv \frac{\left| \int d\omega_1 d\omega_2 |f_s(\omega_1)|^2 |\Phi(\omega_1, \omega_2)|^2 e^{i\omega_1\Delta_s} e^{i\omega_2\Delta_i} \right|}{\int d\omega_1 d\omega_2 |f_s(\omega_1)|^2 |\Phi(\omega_1, \omega_2)|^2}. \end{aligned} \quad (10)$$

Let us assume a Gaussian shape for $f_s(\omega_1)$:

$$f_s(\omega_1) = \exp[-(\omega_1 - \omega_{10})^2 / 2\sigma_f^2] \quad (11)$$

with a width of σ_f . We can assume for simplicity the phase match factor in $\Phi(\omega_1, \omega_2)$ also has a Gaussian shape as $F(\omega_1, \omega_2) = \exp[-(\omega_1 - \omega_2)^2 / 2\sigma_0^2]$ with a width of σ_0 . Then, after shifting to center frequencies of all fields with $\Omega_j \equiv \omega_j - \omega_{j0}$ ($j = 1, 2$), we have

$$\begin{aligned} |f_s(\omega_1)\Phi(\omega_1, \omega_2)|^2 &= \exp\left(-\frac{\Omega_1^2}{\sigma_f^2}\right) \exp\left[-\frac{(\Omega_1 + \Omega_2)^2}{2\sigma_p^2}\right] \\ &\quad \times \exp\left[-\frac{(\Omega_1 - \Omega_2)^2}{\sigma_0^2}\right]. \end{aligned} \quad (12)$$

From Eq.(10), we obtain

$$\mathcal{V}(\Delta_s, \Delta_i) = \exp[-Q(\Delta_s, \Delta_i)/4], \quad (13)$$

with

$$\begin{aligned} Q(\Delta_s, \Delta_i) &\equiv \frac{2\Delta_i^2\sigma_p^2\sigma_0^2}{2\sigma_p^2 + \sigma_0^2} + \left(\Delta_s - \frac{\sigma_0^2 - 2\sigma_p^2}{\sigma_0^2 + 2\sigma_p^2}\Delta_i\right)^2 \\ &\quad \times \frac{\sigma_0^2 + 2\sigma_p^2}{4 + (\sigma_0^2 + 2\sigma_p^2)/\sigma_f^2}. \end{aligned} \quad (14)$$

The visibility expression in Eq.(13) can explain the results in Fig.2. For Trace (i) in Fig.2, the idler path is balanced with $\Delta_i = 0$, but signal field has delay Δ_s . Then we have

$$\mathcal{V}_1(\Delta_s) = \exp[-\Delta_s^2/4T_s^2], \quad (15)$$

with

$$T_s^2 \equiv \frac{1}{\sigma_f^2} + \frac{4}{\sigma_0^2 + 2\sigma_p^2}. \quad (16)$$

The solid curve for Trace (i) of Fig.2 is a plot of Eq.(15) as a function of $1/\sigma_f$ with $\sigma_p = 0.28$ rad/ps, $\sigma_0 = 4.8$ rad/ps taken from experimental parameters (see Supplementary Materials IV-A). Note that Eq.(16) is actually the coherence time of the signal field after the filter. To see better the physical meaning of Eq.(16), we rewrite it in terms of $T_f \equiv 1/\sigma_f$, $T_0 \equiv 1/\sigma_0$, and the coherence time $T_p \equiv 1/\sigma_p$ of the pump field:

$$T_s^2 = T_f^2 + T_c^2 \quad (17)$$

with $T_c^2 \equiv 4T_p^2T_0^2/(2T_0^2 + T_p^2)$ as the coherence time of the generated signal field without filter. Note that Eq.(17) has the same form as Eq.(2) for the classical interferometer so T_s depends highly on T_f , the reciprocal width of the filter, and is dominated by T_f for narrow filter width $\sigma_f \rightarrow 0$ but reaches T_c for no filtering. This indicates that optical filtering of the signal field can increase the coherence time of the signal field, which is the same as the classical interferometer. This is not surprising because $\Delta_i = 0$ corresponding to the case in Eq.(5) as discussed earlier and $\mathcal{C} = 0$ or Eq.(3) becomes Eq.(1) with equal sign for classical case.

However, as Δ_i becomes non-zero and is large enough so that $|i_1\rangle$ and $|i_2\rangle$ are well separated, the visibility is nearly zero independent of filtering, as shown in the red points of Fig.2 and the solid curve of Trace (iii) obtained from Eq.(13) with $\Delta_i = 10ps$ but σ_p, σ_0 kept the same as before. The intermediate case of green points and Trace (ii) is for $\Delta_i = 5ps$. It can be seen that the theoretical prediction from Eq.(13) fits experimental data very well.

As another test of Eq.(3), we consider an extreme case of $\mathcal{D} = 0$ by setting $\Delta_s = 0$ with balanced signal path so that signal photon wavepackets overlap in time and become completely indistinguishable in its generation from either PA1 or PA2. One may think filtering at signal field would have no effect on interference since we already have complete indistinguishability for the signal photon. However, because of the quantum correlation between the signal and idler photons, filtering at signal field may alter the idler field and according to the discussion on the state in Eq.(4), this will change the entanglement property between the signal and idler fields, which, in other words, is concurrence \mathcal{C} . This will change interference visibility \mathcal{V} according to Eq.(3), as we will see in the following.

When $\Delta_s = 0$, we have from Eq.(14)

$$\mathcal{V}_2(\Delta_i) = \exp[-\Delta_i^2/4T_i^2] \quad (18)$$

with

$$\begin{aligned} T_i^2 &\equiv \frac{\sigma_0^2 + 2\sigma_p^2 + 4\sigma_f^2}{\sigma_f^2(\sigma_0^2 + 2\sigma_p^2) + 2\sigma_p^2\sigma_0^2} \\ &= \frac{2T_f^2T_0^2 + 4T_0^2T_p^2 + T_f^2T_p^2}{2T_f^2 + 2T_0^2 + T_p^2}. \end{aligned} \quad (19)$$

Now let us try to understand Eq.(19) in the language of Eq.(3). As said earlier, $\Delta_s = 0$ corresponds to $\mathcal{D} = 0$ and Eq.(3) becomes

$$\mathcal{V}^2 + \mathcal{C}^2 = 1. \quad (20)$$

Now \mathcal{C} plays a similar role as \mathcal{D} in Eq.(1) with equal sign. In this case, \mathcal{C} can be altered by delay Δ_i of the idler field, as we discussed for Eq.(4). Delay Δ_i controls the overlap $\cos\theta = |\langle i_1 | i_2 \rangle|$ of the two idler fields and then the degree of entanglement: $\Delta_i = 0$ leads to product state with no entanglement while large Δ_i may give maximum entanglement with concurrence $\mathcal{C} = 1$. This is reflected directly in Eq.(18) and the size of relevant Δ_i is determined by T_i in Eq.(19), which depends on the filter bandwidth σ_f .

There are two notable limiting cases with simple physical pictures. For narrow band pumping ($\sigma_p \ll \sigma_f, \sigma_0$), $T_i \rightarrow \sqrt{T_f^2 + 4T_0^2}$, which is similar to T_s in Eq.(17) or classical coherence time in Eq.(2) and strongly depends on T_f for narrow filtering of the signal field. Perhaps it is easier to understand this case in the extreme case of CW pumping with $\sigma_p = 0$. Under this condition, the frequencies of signal and idler photons are perfectly anti-correlated: $\omega_s + \omega_i = 2\omega_{p0}$ so filtering signal field is equivalent to filtering the idler field and will also narrow the idler bandwidth and therefore changes T_i in the same way. That is why T_i in this case has the same form as T_s in Eq.(17) or the classical coherence time in Eq.(2). Filtering can change \mathcal{C} and thus \mathcal{V} , in a similar way to \mathcal{D} in Eq.(1).

On the other hand, for broad band pumping ($\sigma_f \ll \sigma_p, \sigma_0$), $T_i \rightarrow \sqrt{T_p^2/2 + T_0^2} \equiv \bar{T}_i$, which hardly depends on σ_f , the width of the filter. In this limiting case, the broad band pumping results in imperfect frequency correlation between signal and idler. Thus optical filtering for the signal field does not significantly change the spectral/temporal property of the correlated idler fields or the overlap $\cos\theta$ of the two idler fields, which is mainly determined by the pump bandwidth σ_p and phase matching bandwidth σ_0 .

The intermediate case of finite pumping bandwidth can be fully described by Eq.(19). To verify it, we measure T_i for three bandwidths of pumping as a function of the filter bandwidth. T_i is obtained by measuring visibility versus delay Δ_i and fitting Eq.(18) (see Supplementary Materials IV-B and IV-C for details). The results are shown in Fig.3 and the experimental data fit the theory quite well. As a comparison, we also plot T_s (brown), which is the same as T_i in the limit of $\sigma_p = 0$ and linearly depends on $1/\sigma_f$. As the pump bandwidth increases, T_i deviates from this linear dependence more and more.

In summary, by investigating how optical filtering can affect the performance of an unbalanced pulsed SU(1,1) quantum interferometer, we find that quantum entanglement plays a similar role as distinguishability in changing the visibility of interference. On the other hand, this connection between interference visibility and quantum en-

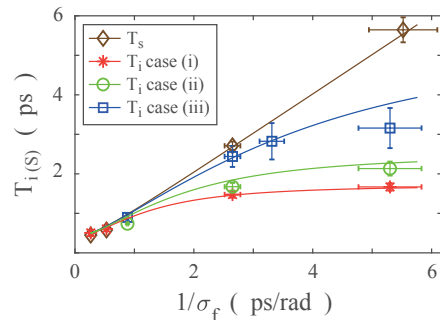


FIG. 3. T_i as a function of reciprocal bandwidth $1/\sigma_f$ of the signal field filter for (i) $\sigma_p = 0.80nm$, (ii) $\sigma_p = 0.60nm$, and (iii) $\sigma_p = 0.24nm$. T_s is also plotted from Eq.(16) together with measured data, corresponding to $\sigma_p = 0$ for T_i .

tanglement can be used to characterize quantum entanglement from measured visibility for some systems that are hard to access²⁷.

It should be noted that our discussion about the relation between interference and entanglement is based on a single-mode description of the system. For the multi-mode description of experiment given in Eq.(6), however, although visibility of interference can be derived and matches the experimental data very well, the simple physical interpretation in the language of Eq.(3) does not apply because it is a challenge to obtain concurrence \mathcal{C} for a multi-mode system.

On the other hand, if the joint spectral function $\Phi(\omega_1, \omega_2)$ is factorized so that the fields can be described by single temporal modes, it is equivalent to a single-mode system and can be described in the language of Eq.(3). This is the case when $\sigma_f \rightarrow 0$ or in the limit of large $1/\sigma_f$ in Fig.2. In this case, we can show (see Supplementary Materials III) $\mathcal{C}^2 = 1 - \exp(-\Delta_i^2/2\bar{T}_i^2)$. Combining with visibility in Eq.(19) in the limit of $\sigma_f \rightarrow 0$, we find \mathcal{C} and \mathcal{V} satisfy Eq.(20), which is a result of Eq.(3) when noticing that the limit of large $1/\sigma_f$ means temporal indistinguishability, i.e., $\mathcal{D} = 0$, just like the single-mode discussion.

This work was supported in part by National Natural Science Foundation of China (Grants No. 91836302, No. 12004279, and No. 12074283)

¹N. Bohr in *Quantum Theory and Measurement*, ed. J. A. Wheeler and W. H. Zurek (Princeton University Press, 1983).

²B. -G. Englert, "Fringe Visibility and Which-Way Information: An Inequality," *Phys. Rev. Lett.* **77**, 2154 (1996).

³S. Dürr, T. Nonn, and G. Rempe, "Origin of quantum-mechanical complementarity probed by a 'which-way' experiment in an atom interferometer," *Nature* **395**, 33 (1998).

⁴M. O. Scully and K. Drühl, *Phys. Rev. A* **25**, 2208 (1982).

⁵M. O. Scully, B.-G. Englert, and H. Walther, "Quantum Optical Tests of Complementarity," *Nature* **351**, 111 (1991).

⁶M. Born and E. Wolf, *Principle of Optics*, Pergamon Press, 1st ed., 1959; 6th ed., 1980.

⁷X.-F. Qian, T. Malhotra, A. N. Vamivakas, and J. H. Eberly, "Coherence constraints and the last hidden optical coherence," *Phys. Rev. Lett.* **117**, 153901 (2016).

- ⁸X.-F. Qian, A. N. Vamivakas, and J. H. Eberly, “Entanglement limits duality and vice versa,” *Optica* **5**, 942 (2018).
- ⁹X.-F. Qian, K. Konthasinghe, S. K. Manikandan, D. Specker, A. N. Vamivakas, and J. H. Eberly, “Turning off quantum duality,” *Phys. Rev. Res.* **2**, 012016(R) (2020).
- ¹⁰X. Y. Zou, L. J. Wang, and L. Mandel, “Induced coherence and indistinguishability in optical interference,” *Phys. Rev. Lett.* **67**, 318 (1991).
- ¹¹A. G. Zajonc, L. J. Wang, X. Y. Zou, and L. Mandel, “Quantum eraser,” *Nature* **353**, 507 (1991).
- ¹²Armin Hochrainer, Mayukh Lahiri, Manuel Erhard, Mario Krenn, and Anton Zeilinger, “Quantum Indistinguishability by Path Identity: The awakening of a sleeping beauty”, *Rev. Mod. Phys.*, in press (2021). arXiv:2101.02431.
- ¹³B. Yurke, S. L. McCall, and J. R. Klauder, “SU(2) and SU(1,1) interferometers,” *Phys. Rev. A* **33**, 4033 (1986).
- ¹⁴M. V. Chekhova and Z. Y. Ou, “Nonlinear interferometers in quantum optics,” *Adv. in Opt. and Photonics* **8**, 104 (2016).
- ¹⁵G. B. Lemos, V. Borish, G. D. Cole, S. Ramelow, R. Lapkiewicz, and A. Zeilinger, “Quantum imaging with undetected photons,” *Nature* **512**, 409 (2014).
- ¹⁶D. A. Kalashnikov, A. V. Paterova, S. P. Kulik, and L. A. Krivitsky, “Infrared spectroscopy with visible light,” *Nat. Photonics* **10**, 98 (2015).
- ¹⁷A. V. Paterova, S. M. Maniam, H. Yang, G. Grenci, and L. A. Krivitsky, “Hyperspectral infrared microscopy with visible light,” *Science Advances* **6**, eabd0460 (2020).
- ¹⁸Mirco Kutas, Björn Haase, Patricia Bickert, Felix Riexinger, Daniel Molter, and Georg von Freymann, “Terahertz quantum sensing,” *Science Advances* **6**, 8065 (2020).
- ¹⁹T. Sh. Iskhakov, S. Lemieux, A. Perez, R. W. Boyd, G. Leuchs, and M. V. Chekhova, “Nonlinear interferometer for tailoring the frequency spectrum of bright squeezed vacuum,” *J. Mod. Opt.* **63**, 64 (2015).
- ²⁰J. Su, L. Cui, J. Li, Y. Liu, X. Li, and Z. Y. Ou, “Versatile and precise quantum state engineering by using nonlinear interferometers,” *Opt. Express* **27**, 20479 (2019).
- ²¹L. Cui, J. Su, J. Li, Y. Liu, X. Li, and Z. Y. Ou, “Quantum state engineering by nonlinear quantum interference,” *Phys. Rev. A* **102** 033718 (2020).
- ²²Y. Shaked, Y. Michael, R. Z. Vered, L. Bello, M. Rosenbluh, and A. Pe’er, “Lifting the bandwidth limit of optical homodyne measurement with broadband parametric amplification,” *Nat. Commun.* **9**, 609 (2018).
- ²³Jiamin Li, Yuhong Liu, Nan Huo, Liang Cui, Chang Feng, Z. Y. Ou, and Xiaoying Li, “Pulsed entanglement measured by parametric amplifier assisted homodyne detection,” *Optics Express* **27** 30552 (2019).
- ²⁴Jiamin Li, Yuhong Liu, Nan Huo, Liang Cui, Sheng Feng, Xiaoying Li, and Z. Y. Ou, “Measuring continuous-variable quantum entanglement with parametric amplifier assisted homodyne detection,” *Phys. Rev. A*, **101**, 053801 (2020).
- ²⁵Z. Y. Ou and Xiaoying Li, “Quantum SU(1,1) interferometers: Basic principles and applications,” *APL Photonics* **5**, 080902 (2020).
- ²⁶J. Chen, X. Li, and P. Kumar, “Two-photon-state generation via four-wave mixing in optical fibers,” *Phys. Rev. A* **72**, 033801 (2005).
- ²⁷Carlos Sánchez Muñoz and Frank Schlawin, “Photon Correlation Spectroscopy as a Witness for Quantum Coherence,” *Phys. Rev. Lett.* **124**, 203601 (2020).